



HAL
open science

Identification of recessive lethal alleles in the diploid genome of a candida albicans laboratory strain unveils a potential role of repetitive sequences in buffering their deleterious impact.

Timea Marton, Adeline Feri, Pierre-Henri Commere, Corinne Maufrais,
Christophe d'Enfert, Mélanie Legrand

► To cite this version:

Timea Marton, Adeline Feri, Pierre-Henri Commere, Corinne Maufrais, Christophe d'Enfert, et al.. Identification of recessive lethal alleles in the diploid genome of a candida albicans laboratory strain unveils a potential role of repetitive sequences in buffering their deleterious impact.. MSphere, 2019, 4 (1), pp.e00709-18. 10.1128/mSphere.00709-18 . hal-02619101

HAL Id: hal-02619101

<https://hal.inrae.fr/hal-02619101>

Submitted on 25 May 2020

HAL is a multi-disciplinary open access archive for the deposit and dissemination of scientific research documents, whether they are published or not. The documents may come from teaching and research institutions in France or abroad, or from public or private research centers.

L'archive ouverte pluridisciplinaire **HAL**, est destinée au dépôt et à la diffusion de documents scientifiques de niveau recherche, publiés ou non, émanant des établissements d'enseignement et de recherche français ou étrangers, des laboratoires publics ou privés.



Distributed under a Creative Commons Attribution 4.0 International License



Identification of Recessive Lethal Alleles in the Diploid Genome of a *Candida albicans* Laboratory Strain Unveils a Potential Role of Repetitive Sequences in Buffering Their Deleterious Impact

Timea Marton,^{a,b} Adeline Feri,^{a,b*} Pierre-Henri Commere,^c Corinne Maufrais,^{a,d} Christophe d'Enfert,^a Melanie Legrand^a

^aInstitut Pasteur, INRA, Unité Biologie et Pathogénicité Fongiques, Paris, France

^bUniversité Paris Diderot, Sorbonne Paris Cité, Cellule Pasteur, Paris, France

^cInstitut Pasteur, Unité de Technologie et de Service Cytométrie et Biomarqueurs, Plate-Forme Cytométrie, Paris, France

^dCentre de Bioinformatique, Biostatistique et Biologie Intégrative (C3BI), USR 3756 IP CNRS, Institut Pasteur, Paris, France

ABSTRACT The heterozygous diploid genome of *Candida albicans* is highly plastic, with frequent loss of heterozygosity (LOH) events. In the SC5314 laboratory strain, while LOH events are ubiquitous, a chromosome homozygosity bias is observed for certain chromosomes, whereby only one of the two homologs can occur in the homozygous state. This suggests the occurrence of recessive lethal allele(s) (RLA) preventing large-scale LOH events on these chromosomes from being stably maintained. To verify the presence of an RLA on chromosome 7 (Chr7), we utilized a system that allows (i) DNA double-strand break (DSB) induction on Chr7 by the I-SceI endonuclease and (ii) detection of the resulting long-range homozygosity. I-SceI successfully induced a DNA DSB on both Chr7 homologs, generally repaired by gene conversion. Notably, cells homozygous for the right arm of Chr7B were not recovered, confirming the presence of RLA(s) in this region. Genome data mining for RLA candidates identified a premature nonsense-generating single nucleotide polymorphism (SNP) within the HapB allele of C7_03400c whose *Saccharomyces cerevisiae* ortholog encodes the essential Mtr4 RNA helicase. Complementation with a wild-type copy of *MTR4* rescued cells homozygous for the right arm of Chr7B, demonstrating that the *mtr4*^{K880*} RLA is responsible for the Chr7 homozygosity bias in strain SC5314. Furthermore, we observed that the major repeat sequences (MRS) on Chr7 acted as hot spots for interhomolog recombination. Such recombination events provide *C. albicans* with increased opportunities to survive DNA DSBs whose repair can lead to homozygosity of recessive lethal or deleterious alleles. This might explain the maintenance of MRS in this species.

IMPORTANCE *Candida albicans* is a major fungal pathogen, whose mode of reproduction is mainly clonal. Its genome is highly tolerant to rearrangements, in particular loss of heterozygosity events, known to unmask recessive lethal and deleterious alleles in heterozygous diploid organisms such as *C. albicans*. By combining a site-specific DSB-inducing system and mining genome sequencing data of 182 *C. albicans* isolates, we were able to ascribe the chromosome 7 homozygosity bias of the *C. albicans* laboratory strain SC5314 to an heterozygous SNP introducing a premature STOP codon in the *MTR4* gene. We have also proposed genome-wide candidates for new recessive lethal alleles. We additionally observed that the major repeat sequences (MRS) on chromosome 7 acted as hot spots for interhomolog recombination. Maintaining MRS in *C. albicans* could favor haplotype exchange, of vital importance to LOH events, leading to homozygosity of recessive lethal or deleterious alleles that inevitably accumulate upon clonality.

Citation Marton T, Feri A, Commere P-H, Maufrais C, d'Enfert C, Legrand M. 2019. Identification of recessive lethal alleles in the diploid genome of a *Candida albicans* laboratory strain unveils a potential role of repetitive sequences in buffering their deleterious impact. mSphere 4:e00709-18. <https://doi.org/10.1128/mSphere.00709-18>.

Editor Aaron P. Mitchell, Carnegie Mellon University

Copyright © 2019 Marton et al. This is an open-access article distributed under the terms of the [Creative Commons Attribution 4.0 International license](https://creativecommons.org/licenses/by/4.0/).

Address correspondence to Melanie Legrand, melanie.legrand@pasteur.fr.

* Present address: Adeline Feri, Pathoquest, BioPark, Paris, France.

Received 25 December 2018

Accepted 24 January 2019

Published 13 February 2019

KEYWORDS *Candida albicans*, homologous recombination, loss of heterozygosity, major repeat sequences, recessive lethal alleles

In diploid genomes, new mutations are heterozygous, and their effect is generally masked by the presence of the ancestral allele. As claimed in Haldane's sieve, only mutations that confer a fitness advantage as heterozygotes can invade the population. Although true, it does not make specific prediction about the fitness of the mutant homozygotes. Recent studies of *Saccharomyces cerevisiae* have observed maintenance of genetic variation due to heterozygote advantage, as a result of overdominance of mutated alleles (1). In addition, Gerstein and colleagues used the model organism *S. cerevisiae* to show that recessive beneficial mutations can avoid Haldane's sieve in clonal organisms, through rapid loss of heterozygosity (LOH), and thus contribute to rapid evolutionary adaptation (1). Similarly, in *Candida albicans*, mutations followed by genomic rearrangements such as LOH events and isochromosome formation have been associated with the acquisition of antifungal resistance (2, 3), bringing forth the idea that mechanisms favoring genome plasticity could contribute to *C. albicans* fitness within the host and upon exposure to antifungal agents. *C. albicans* is a frequent human commensal yeast responsible for both mucosal fungal infections and the majority of life-threatening nosocomial fungal infections (4). Its diploid genome displays a high degree of plasticity that includes, in particular, LOH events. Despite frequent LOH, overall heterozygosity is maintained in the *C. albicans* population, as illustrated by various studies that highlighted the elevated levels of natural heterozygosity, with a heterozygous position every ~200 to 250 bp on average (5–7). Furthermore, several studies revealed that genome heterozygosity showed a significant correlation with higher growth rates (6, 8, 9).

Essentially, mutations can be categorized as beneficial, harmful, or neutral and can be differently assigned depending on the organism's environment. Because the mode of reproduction of *C. albicans* is mainly clonal, and therefore mimics inbreeding in higher eukaryotes, an increased number of recessive lethal alleles (RLA) in the *C. albicans* genome is expected compared to other eukaryotes that undergo true sexual reproduction. Various types of mutations can impact the functionality of alleles and render them inactive; however, mutations introducing premature STOP codons would convey the most obvious effect. Within the *C. albicans* laboratory strain SC5314, Muzzey et al. (10) reported almost 200 genes for which one of the alleles contains a single nucleotide polymorphism (SNP) that introduces a premature STOP codon. Functional differences have already been reported for the two alleles of a heterozygous gene, and in all instances, the effect of the recessive mutation was visible only upon homozygosis toward the mutated allele (*HIS4* [11], *MBP1* [12], *GPI16/MRF2* [13]). Moreover, SNPs in promoter regions have been shown to alter expression regulation of two alleles (14). Of interest, LOH is pervasive in *C. albicans* isolates, as homozygous regions can be found in all sequenced isolates and affect all of the chromosomes. These LOH events vary in size: they can be limited to a single chromosomal region, affect an entire chromosomal arm, or even cover the entire chromosome (6, 7, 9).

Recently, a combination of molecular tools has been developed to study genome dynamics in *C. albicans*. First, an LOH reporter system takes advantage of fluorescent markers at an artificial heterozygous locus containing the BFP and GFP genes (15). Consequently, the appearance of spontaneous LOH events for the given locus can be monitored by the fluorescent status of cells using flow cytometry (15). Second, LOH events are often a result of DNA double-strand breaks (DSB) (16) resolved by means of various DNA repair mechanisms which can either be independent or dependent of homologous recombination. Feri et al. (13) developed an inducible, locus-specific DNA DSB system that uses the I-SceI meganuclease from *S. cerevisiae*. When coupled to the BFP/GFP LOH reporter system, this system can be used to study the consequence of a targeted DNA DSB on the appearance of LOH events. Indeed, Feri et al. (13) have shown that I-SceI-induced DNA breaks are predominantly repaired by gene conversion result-

ing in limited LOH. Nevertheless, various patterns of long-range LOH can also be obtained. Of note, the engineered system, alongside sequence resources, helped identify a RLA on Chr4B of *C. albicans* strain SC5314 (13). This RLA is the consequence of a nonsense mutation in the *GPI16* gene that encodes an essential component of the glycosylphosphatidylinositol (GPI) anchor biosynthetic machinery and explains why Chr4B is never observed in the homozygous state in *C. albicans* strains SC5314. Notably, this RLA appeared unique to strain SC5314 (13).

Although LOH can be observed on all eight chromosome pairs, prior studies conducting haplotype characterization of (i) progeny from the parasexual life cycle (17), (ii) homozygous diploid isolates derived from *RAD52* double knockout mutants (18), and (iii) haploid strains of *C. albicans* (8) showed a chromosome homozygosity bias in the *C. albicans* laboratory strain SC5314. This suggests that mutations, potentially RLAs, could apply constraints on the directionality of LOH events. Indeed, the homozygosity state of some chromosomes was observed only for a given homolog while recurrently absent for the other homolog. This is the case for chromosomes 1, 4, 6, as well as chromosome 7 (Chr7) for which homozygosity of haplotype B (HapB) is never observed, while haplotype A homozygosity is, suggesting the presence of RLAs on Chr7 HapB (Chr7B).

In this study, we aimed to identify the RLA(s) on Chr7B using an approach similar to that developed by Feri et al. (13) when searching for RLAs on Chr4B. This approach also allowed addressing the role that repetitive sequences, such as the major repeat sequences (MRS), might play on the overall genome dynamics of *C. albicans*. MRS are unique to *C. albicans* and *Candida dubliniensis*, and are found throughout their genomes. MRS are composed of three subregions: RB2 which contains the *FRG8* gene, the RPS region which varies in repeat numbers (and thus, in size), and the HOK region. *C. albicans* possesses eight MRS, one on each chromosome with the exceptions of Chr7 where the presence of one MRS on each arm is observed and of Chr3 where an incomplete MRS is located (19). MRS expansion and contraction have previously been shown to be involved in chromosome loss where the chromosome copy containing the shorter MRS region is spontaneously lost (20). Furthermore, MRS have also been shown to be involved in chromosome translocation (19), when two different chromosomes exchange large regions of an arm. Results presented below confirm that homozygosity of Chr7B is not recovered and that this is the consequence of a premature STOP codon in the Chr7B-borne allele of the RNA helicase-encoding gene *MTR4*. Furthermore, we highlight that repeat regions such as MRS are hot spots for interhomolog recombination upon DNA repair and play a role in LOH dynamics in *C. albicans*.

RESULTS

Strain engineering to promote and detect long-range LOH on Chr7. Genome analysis revealed that the left arm of Chr7 carries only 9 heterozygous SNPs in 3 ORFs, while the right arm of Chr7 carries 784 heterozygous SNPs in 105 ORFs. Because RLAs are more likely to be found in heterozygous regions, we focused on the right arm of Chr7 to understand Chr7 homozygosity bias. To efficiently screen for the presence of RLAs on Chr7 right arm, we engineered strains carrying an artificial heterozygous BFP/GFP LOH reporter system (15) associated with an I-SceI DNA DSB-inducing system (13) (Fig. 1A). Because we chose to insert the I-SceI target site (TS) associated with the auxotrophic marker *URA3* conferring uridine prototrophy in the most *mrs-7b* proximal, gene-free region found on the right arm of Chr7, this setup allows rendering a maximum number of alleles homozygous on this arm while avoiding *mrs-7b*. Integration of the *URA3*-I-SceI TS cassette can occur on either Chr7 homologs (Chr7A or Chr7B); thus, transformants were screened by SNP-RFLP to identify which Chr7 haplotype was targeted (see Fig. S1 in the supplemental material). Using the heterozygous SNP at position 727,328, we showed that 28/51 *C. albicans* transformants had integrated the I-SceI TS on Chr7A (55%) and 23/51 on Chr7B (45%), demonstrating the absence of integration bias for this locus. Two independent transformants that had integrated the

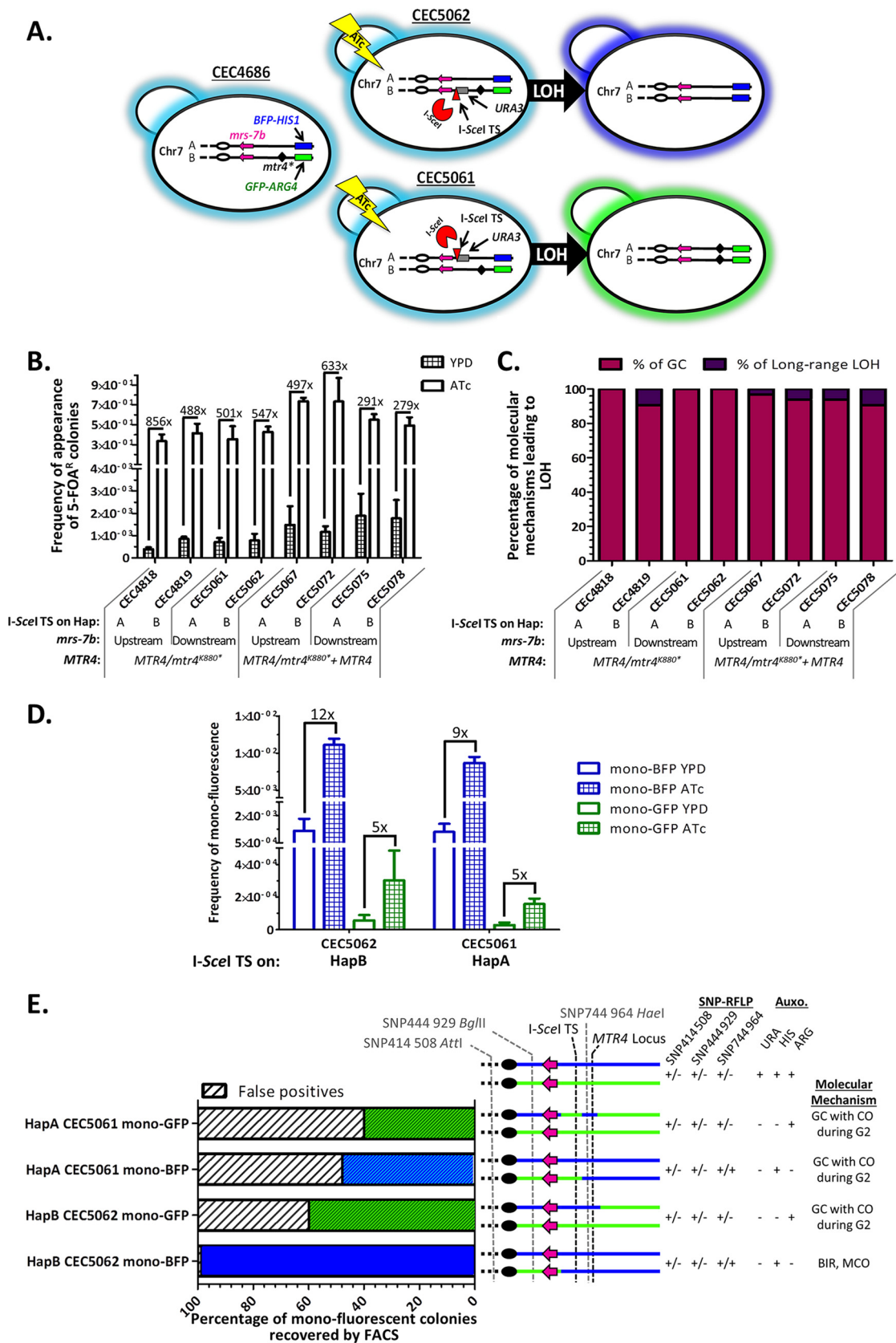


FIG 1 Coupling of a DNA double-strand-break-inducing system and a FACS-optimized LOH reporter system on Chr7. (A) Illustration of strains bearing the BFP/GFP LOH reporter system on the right arm of Chr7 associated with an I-SceI-inducible DNA DSB system on Chr7B (CEC5062) or Chr7A (CEC5061). Upon addition of ATc, the mega-endonuclease I-SceI is expressed and will generate a DNA DSB (Continued on next page)

I-SceI TS on Chr7 HapA (CEC5061) or HapB (CEC5062), were selected and used in subsequent analysis (Fig. 1A).

Strains CEC5061 and CEC5062 underwent preliminary characterization regarding their fluorescence status, as well as their growth rate to ensure that the successive transformation steps did not significantly alter their fitness. The fluorescence status of the intermediate and final strains was verified by flow cytometry. The flow cytometry outputs clearly displayed (i) the absence of fluorescence signals in the parental strain CEC4591, (ii) a shift toward the mono-GFP gate upon integration of the P_{TDH3} -GFP-ARG4 cassette in CEC4679, (iii) a shift toward the double-fluorescent BFP/GFP gate upon integration of the P_{TDH3} -BFP-HIS1 cassette in CEC4685, and (iv) the double-fluorescence status of the population upon integration of the URA3-I-SceI-TS cassette in strains CEC5061 and CEC5062 (Fig. S2A).

Growth curves performed demonstrated that only the insertion of the URA3-I-SceI TS cassette in strains CEC5061 and CEC5062 resulted in a higher growth rate, almost certainly due to the uridine prototrophy in these strains, as URA3 deletion has been shown to result in significant decreases in *C. albicans* growth rate even when *ura3Δ* strains are grown in rich medium (21) (Fig. S2B).

Validation of the I-SceI DNA DSB induction system on Chr7 by 5-FOA counter-selection. As the I-SceI TS is associated with the genetic auxotrophic marker URA3, we could assess the frequency of cells that have survived an I-SceI-induced DNA DSB at the TS by monitoring the frequency of appearance of 5-fluoroorotic acid-resistant (5-FOA^R) colonies upon I-SceI induction. Indeed, 5-FOA^R colonies should have lost the URA3 genetic marker (uridine auxotrophy) and are likely to represent cells that have sustained an I-SceI-dependent DNA DSB through a LOH event, even though point mutations in the URA3 gene cannot be excluded. We obtained 501 times more 5-FOA^R colonies after I-SceI induction when the I-SceI TS was located on Chr7A and 547 times more 5-FOA^R colonies when the I-SceI TS was located on Chr7B (Fig. 1B). These data confirmed the efficiency of the I-SceI-dependent DNA DSB induction system on Chr7. The majority of I-SceI DNA DSB-induced 5-FOA^R colonies (90 to 100%) resulted from DNA DSB repair by gene conversion, as suggested by fluorescence and auxotrophy profiles of 32 Ura⁻ colonies (Fig. 1C). Similar to what has been observed for Chr4 (13), DNA DSBs by I-SceI on Chr7 are predominantly repaired by gene conversion repair mechanisms, resulting in short-range LOH events.

An I-SceI-induced DNA DSB on Chr7B leads to viable cells homozygous for the right arm of Chr7A. Although the 5-FOA assays yield information on the overall occurrence of LOH events encompassing the URA3 gene, it does not allow us to efficiently study the underrepresented long-range LOH events. Thus, we also investigated LOH frequency upon I-SceI expression using flow cytometry, an assay that specifically detects long-range LOH events. As expected, upon induction of I-SceI in strain CEC5062, possessing the I-SceI TS on the GFP-bearing Chr7B, we observed a

FIG 1 Legend (Continued)

at its target sequence (I-SceI TS linked to the URA3 marker) on Chr7. Theoretically, when the DNA DSB is repaired by break-induced replication or mitotic crossover, doubly fluorescent cells harboring the I-SceI-TS on BFP-bearing Chr7A will become mono-GFP, while doubly fluorescent cells harboring the I-SceI-TS on GFP-bearing Chr7B will become mono-BFP. The centromere (oval), MRS (pink arrow), and candidate RLA (diamond) on Chr7 are shown. (B) Average frequencies of 5-FOA^R colonies obtained after 8 h of I-SceI overexpression and recovery from three independent experiments ($n = 3$) (plus standard deviations [S.D.] [error bars]) alongside fold changes observed between YPD and ATc conditions. (C) Percentage of molecular mechanisms leading to LOH among 5-FOA^R colonies in induced condition ($n = 32$). (D) Histogram representing average frequency ($n = 6$) (plus S.D.) of appearance of monofluorescent cells in the presence (ATc) and absence (YPD) of expression of I-SceI and hence induced DNA DSBs on Chr7B (CEC5062) or Chr7A (CEC5061). Fold changes between uninduced and induced conditions for each monofluorescent population are indicated. (E) Characterization of monofluorescence-sorted individuals ($n = 32$) from induced CEC5062 (I-SceI TS on HapB) and CEC5061 (I-SceI TS on HapA) strains. A subset of sorted individuals was characterized for fluorescence and auxotrophy status in addition to SNP-RFLP for haplotype appointment in order to profile homozygosity of the right arm of Chr7 and determine the molecular mechanism used for I-SceI-induced DNA DSB repair. In the stacked histogram, white and black hatched portions represent missorted cells (false-positive results), while green and blue portions represent the proportions of properly FACS-sorted monofluorescent individuals. The presence of stripes on the green or blue bars indicate that those individuals are not fully homozygous for one given haplotype from the I-SceI TS to the BFP/GFP LOH reporter system on the right arm of Chr7. Abbreviations of molecular mechanisms are as follows; gene conversion (GC), break-induced replication (BIR), mitotic crossover (MCO), gene conversion with crossover (GC with CO).

12-fold increase in the appearance of mono-BFP cells (Fig. 1D). We also observed a fivefold increase in the appearance of mono-GFP cells (Fig. 1D). A subset of each population was recovered by fluorescence-activated cell sorting (FACS) and further characterized. We observed that, while the majority of the mono-BFP population included true mono-BFP cells displaying complete Chr7A homozygosis distal to the I-SceI TS, 100% of the rare true mono-GFP cells displayed only partial homozygosis of Chr7B. From a mechanistic point of view, the mono-BFP cells resulted most likely from the repair of the DNA DSBs by mechanisms of break-induced replication or mitotic crossover, while the mono-GFP cells could be one of the possible outcomes of DNA DSB repair by gene conversion with crossover during the G₂ phase of the cell cycle (Fig. 1E).

Absence of recovery of cells being fully homozygous for the right arm of Chr7B. Unlike targeting the right arm of Chr7B, a DNA DSB on the right arm of Chr7A in strain CEC5061 should lead to a higher increase in frequency of the mono-GFP cells compared to the mono-BFP cells (Fig. 1D). Although an augmentation in frequency of both mono-BFP and mono-GFP cells was obtained, the mono-BFP cells still appeared at a higher frequency, 8×10^{-3} ($\pm 8 \times 10^{-4}$), compared to 1×10^{-4} ($\pm 3 \times 10^{-5}$) for the mono-GFP cells in the induced condition (Fig. 1D). Characterization of a subset of FACS-sorted mono-BFP cells confirmed that the true mono-BFP cells had arisen from a DNA DSB repaired by gene conversion with crossover during G₂. Further characterization of FACS-sorted mono-GFP cells (corresponding to the expected fluorescence) revealed that the I-SceI-induced homozygosis of Chr7B was only partial in the targeted region. Thus, rather than having experienced break-induced replication or mitotic crossover events extending from the I-SceI site to the BFP/GFP locus, the rare mono-GFP individuals were likely to have resulted from DNA DSB repair by gene conversion with crossover during G₂ (Fig. 1E). In conclusion, we were unable to recover a single individual that had undergone complete homozygosis of the right arm of Chr7B distal to the I-SceI TS. This suggests that complete homozygosis of the right arm of Chr7B is associated with lethality in the SC5314 genetic background, thus confirming the chromosome homozygosis bias previously observed and validating the hypothesis that the presence of RLA(s) in this region could be a cause.

A data mining strategy identifies a heterozygous mutation in the *MTR4* gene as a possible cause of the homozygosis bias of Chr7. Genome sequence data obtained from a collection of 182 *C. albicans* isolates (7), including the reference strain SC5314, was used to compile all heterozygous SNPs within ORFs of Chr7 and search for SNPs (i) generating a premature STOP codon, (ii) showing a heterozygous genotype in SC5314, (iii) never observed in the homozygous state in the collection of 182 genomes, and (iv) located in a coding region never found to be dispensable in *C. albicans*. Only one such SNP was identified, located at position 746,359 on Chr7B. In *C. albicans* strain SC5314, this SNP causes a change from AAA (lysine) on Chr7A to TAA (STOP) on Chr7B in the C7_03400C gene. This gene is the orthologue of *S. cerevisiae* *MTR4* that encodes an essential ATP-dependent RNA helicase involved in RNA processing in *S. cerevisiae* (22–24). In *C. albicans* SC5314, the HapA allele of *MTR4* encodes a full-length Mtr4 protein, while the HapB allele carrying the STOP-introducing SNP encodes a truncated Mtr4^{K880*} protein that misses a C-terminal DSHCT domain, common to DEAD box helicases (Fig. 2A).

The *mtr4*^{K880*} allele is responsible for the Chr7 homozygosis bias. To validate that the identified RLA candidate *mtr4*^{K880*} is truly responsible for the Chr7 homozygosis bias, the full-length *MTR4* ORF was placed ectopically under the control of the P_{T_{DH3}} constitutive promoter in strain CEC5061, giving rise to strain CEC5075 (Fig. 2B). Results shown in Fig. 1B and C confirmed that the DNA DSB-inducing system was functional in this strain and that the I-SceI-induced DNA DSB was predominantly repaired by gene conversion as observed in other instances. Strikingly, flow cytometry analysis revealed a significant elevation in the fold increase of mono-GFP cells obtained upon induction of I-SceI in strain CEC5075 by comparison to CEC5061 (Fig. 2C). Upon cell sorting and characterization of these mono-GFP cells, the majority (93%) appeared

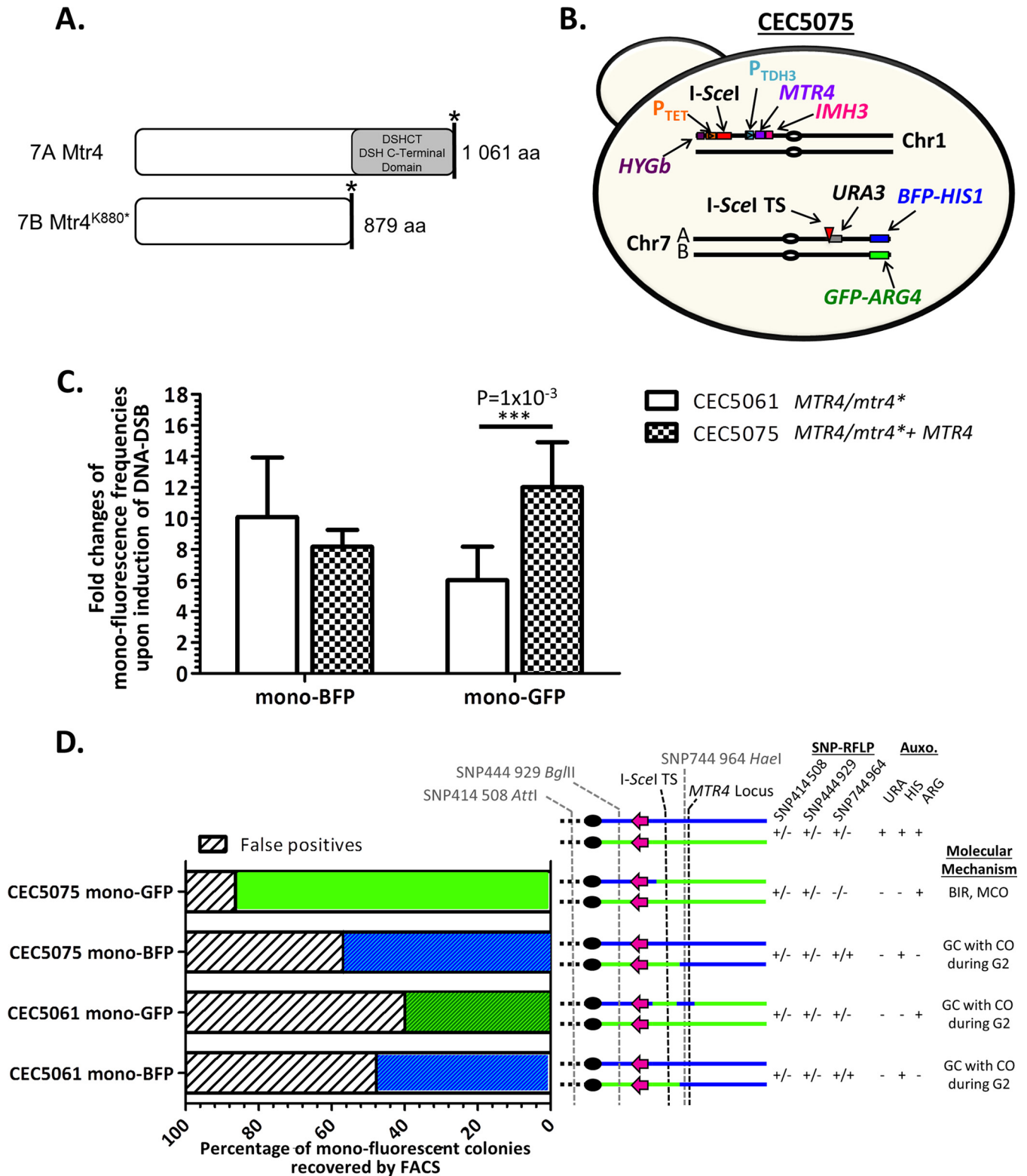


FIG 2 Complementation with a functional *MTR4* allele restores viability of Chr7B homozygous cells. (A) Schematic alignment of the wild-type *MTR4* and *mtr4*^{K880*}-encoded proteins. *MTR4* encodes an ATP-dependent RNA-helicase, and the nonsense mutation in the *mtr4*^{K880*} allele leads to loss of the DSH C-terminal domain shared by DEAD box helicases. aa, amino acids. (B) Illustration of the CEC5075 complemented strain possessing the functional *MTR4* allele at the *RPS1* locus on Chr1. Centromeres are indicated by ovals. (C) Comparison of the average fold increase of the monofluorescent populations upon DNA DSB induction (ATc/YPD) in both parental (CEC5061) and complemented (CEC5075) strains ($n = 6$) (plus S.D.), significance was determined using a bilateral *t* test (P value). (D) Characterization of monofluorescence-sorted individuals ($n = 32$) from induced CEC5061 (I-SceI TS on HapA) and *MTR4*-complemented CEC5075 strains. See the legend to Fig. 1E for explanation.

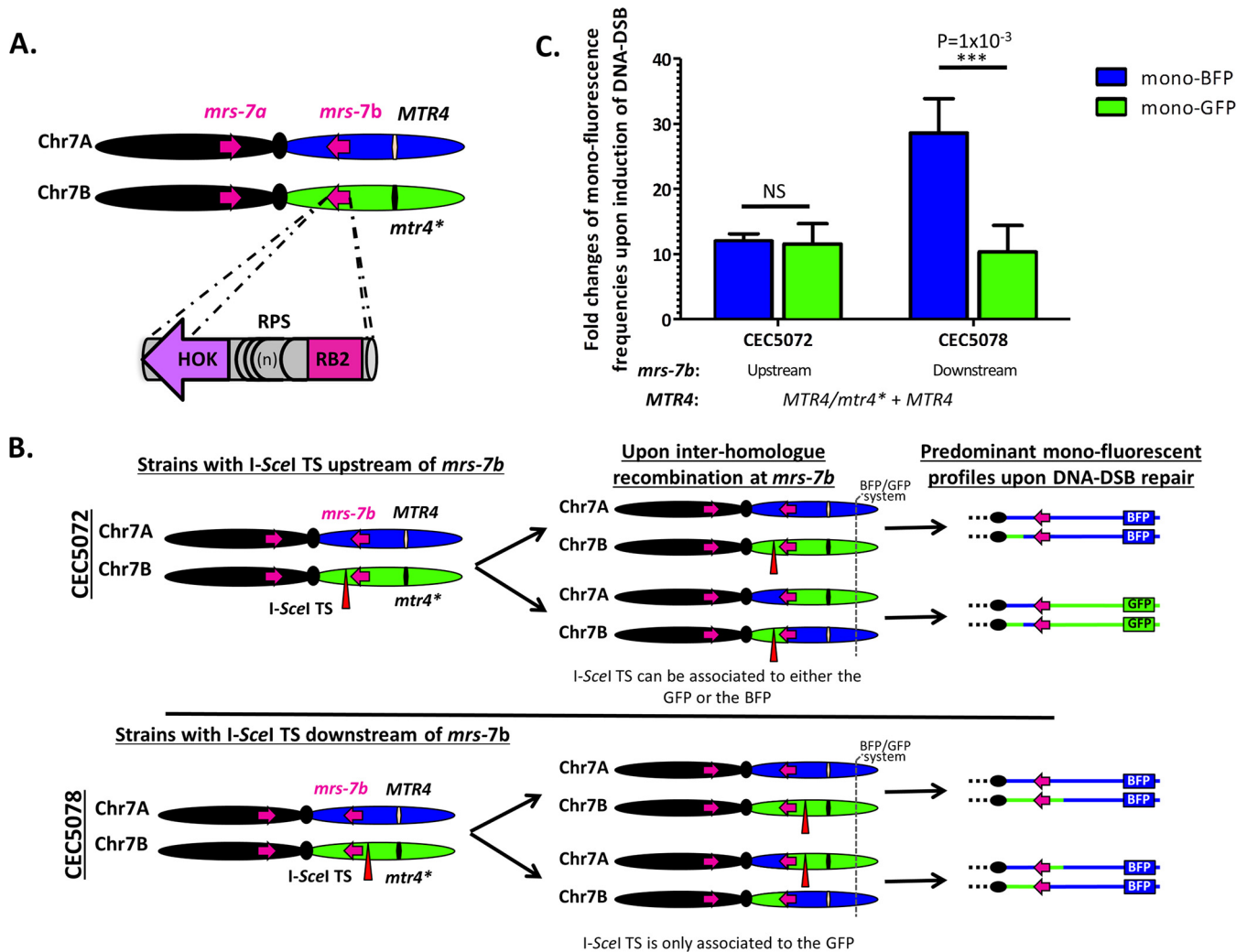


FIG 3 Upon DNA DSB, major repeat sequences are a source of interhomolog recombination. (A) Three subunits compose the MRS, which are hot spots for mitotic crossover. (B) Engineering of strains where the I-SceI TS is located on HapB upstream (CEC5072) or downstream (CEC5078) of *mrs-7b*. Illustration of the right arm of Chr7 upon interhomolog recombination at *mrs-7b* followed by the predominant monofluorescence profiles upon DNA DSB repair leading to long-range LOH events. (C) Histogram showing average fold changes ($n = 6$) (plus S.D.) of monofluorescent populations upon I-SceI induction (ATc versus YPD). While no significant difference in augmentation of both populations is detected when the I-SceI TS is placed upstream of *mrs-7b* (CEC5072), a significant difference is observed when the I-SceI TS is placed downstream of *mrs-7b* (CEC5078). Significance was determined using a bilateral t test (P value).

as true mono-GFP individuals that had become fully homozygous for Chr7B from the I-SceI TS to the BFP/GFP LOH reporter system. These cells were likely to have resulted from the repair of the induced DNA DSB by break-induced replication or mitotic crossover, indicating that complete homozygosis of the right arm of Chr7B is compatible with viability upon addition of a functional *MTR4* allele (Fig. 2D). Similar to what was observed with the CEC5061 parental strain, I-SceI induction in the CEC5075 *MTR4*-complemented strain resulted in an augmentation of mono-BFP cells (Fig. 2C). Eighty-eight percent of these mono-BFP cells corresponded to cells where the DNA DSB had been repaired by gene conversion with crossover during G_2 (Fig. 2D).

Upon DNA DSB, major repeat sequences are a source of interhomolog recombination. Our initial strategy for unveiling RLAs was to induce a DNA DSB downstream of *mrs-7b* (the MRS located on the right arm of Chr7 [Fig. 3A]) in order to ensure that the repeat sequences would not interfere with the DNA repair mechanisms. To seek validation of this initial assumption, the I-SceI TS was moved upstream of *mrs-7b*, between the centromere and *mrs-7b*, on either HapA or HapB and in the presence of an ectopic copy of *MTR4* (Fig. 3B). By plating on 5-FOA-containing medium, we showed

TABLE 1 Summary of chromosome homozygosity bias observed in the literature

Chr	Parasexuality ^a	<i>RAD52</i> mutants ^b	Obligate diploid ^c	Bias summary
R	No BB	No BB		None
1	No AA, no BB	No BB	No BB	BB bias
2	No BB			None
3	No AA	No AA	No BB	None
4	No AA, no BB	No BB	No BB	BB bias
5		No AA		None
6	No BB	No BB	No BB	BB bias
7	No BB	No BB	No BB	BB bias

^aData from reference 17.^bData from reference 18.^cData from reference 8.

that the inducible I-SceI DNA DSB system was functional in the new location and that gene conversion was the preferred mechanism of repair, independently of the targeted haplotype (Fig. 1B and C). Notably, when the I-SceI TS was localized on HapB upstream of *mrs-7b* in an *MTR4*-complemented strain (CEC5072), induction of I-SceI expression resulted in almost equal increases in the mono-GFP and mono-BFP cell populations relative to noninduced conditions (Fig. 3C). This contrasted to what was observed when the I-SceI TS was localized on HapB downstream of *mrs-7b* in an *MTR4*-complemented strain (CEC5078), whereby a greater increase in the mono-BFP cell population than mono-GFP cell population was observed upon I-SceI induction (Fig. 3C). This observation could be explained by interhomolog recombination at *mrs-7b*, which would link the I-SceI TS to either the BFP or GFP markers when the TS is located upstream of *mrs-7b* (Fig. 3B). This would result in equal proportions of mono-BFP and mono-GFP cells upon repair of the I-SceI-induced DNA DSB, keeping in mind that break-induced replication and mitotic crossover are the predominant molecular mechanisms leading to long-range LOH (Fig. 3C). In contrast, when the I-SceI TS is located downstream of *mrs-7b*, it remains linked to the GFP marker, regardless of interhomolog recombination at *mrs-7b*, thus predominantly yielding mono-BFP cells upon I-SceI-induced DNA DSB repair (Fig. 3B and C). Overall, our data suggest that the MRS is a hot spot for interhomolog recombination upon DNA repair on the right arm of Chr7.

Of interest, *C. albicans* Chr7 is characterized by the occurrence of a second MRS on the left arm, namely, *mrs-7a* (Fig. 3A). Strains possessing the I-SceI TS between the centromere and *mrs-7a* and the BFP/GFP LOH reporter system on the left arm of Chr7 also exhibited an equal rate in mono-BFP and mono-GFP cells upon I-SceI induction, whatever the location of the I-SceI TS on HapA or HapB (data not shown), suggesting an increase in the number of cells that have undergone crossover at *mrs-7a*, linking the I-SceI TS to either the BFP or GFP marker. Thus, *mrs-7a* also appears to be a hot spot for interhomolog recombination on Chr7.

DISCUSSION

Previous studies have shown that *C. albicans* strains harbor recessive lethal alleles (RLAs) that are responsible for a bias upon homozygosity of certain chromosomes, whereby only one of the two homologs can be retained in the homozygous state (Table 1). Yet, the nature of these RLAs is generally unknown. In this report, we have ascribed the Chr7 homozygosity bias of the *C. albicans* laboratory strain SC5314 to a heterozygous SNP introducing a premature STOP codon in the *MTR4* gene. Furthermore, we have unveiled the contribution of the major repeat sequence (MRS) to interhomolog recombination and hence, chromosome dynamics in *C. albicans*.

Our work focused on the homozygosity bias observed for Chr7, suggesting the presence of at least one RLA on Chr7B (Table 1). Using a fluorescence-based LOH reporter system and an I-SceI-dependent DNA DSB-inducing system, we have shown that while long-range homozygosity of Chr7A does not affect cell viability, long-range homozygosity of Chr7B is nonviable in *C. albicans* strain SC5314. A library of SNPs compiled from 182 clinical *C. albicans* genomes (7) was searched for SNPs that would

result in the most drastic outcome, i.e., a premature STOP codon. In this respect, we surely underestimated the presence of recessive lethal alleles, as mutations other than premature STOP-introducing SNPs are likely to result in lethal phenotypes. Indeed, nonsynonymous SNPs in coding regions have been shown to negatively impact protein function or regulation (25, 26). Our approach pinpointed an SNP in the *C. albicans* *MTR4* gene that complementation experiments confirmed to be the RLA responsible for the lethality of individuals homozygous for Chr7B in strain SC5314. The identified SNP results in a truncated form of Mtr4 that lacks the last 182 C-terminal amino acids, encompassing a DEAD box family DSHCT domain (Mtr4^{K880*} [Fig. 2A]). In *S. cerevisiae*, *MTR4* encodes an ATP-dependent RNA helicase whose deletion results in nuclear accumulation of unprocessed RNAs (27), and reduction of function results in increased sensitivity to both benomyl and nocodazole (28). Importantly, it has been shown that the C-terminal domain of other fungal RNA helicases is critical for their proper RNA-unwinding function (29), consistent with *mtr4*^{K880*} being a loss-of-function allele and homozygosity of this allele being lethal.

Our study and that of Feri et al. (13) indicate that the mining of the genomes of a large panel of *C. albicans* isolates for premature STOP-introducing SNPs is a suitable approach to identify RLAs responsible for chromosome homozygosity bias in *C. albicans* strains. As a reference, we provide a list of 70 genes that harbor a STOP-introducing SNP in one of the two alleles in the laboratory strain SC5314 in Table S1 in the supplemental material, including 12 alleles (Table 2) that were never found in the homozygous state in a collection of 182 genome-sequenced isolates representative of the *C. albicans* population (7). The locations of these 12 candidate RLAs across the *C. albicans* genome are shown in Fig. 4. Subsequent Sanger sequencing will be necessary to confirm these alleles. Our reduced number of genes with SNPs introducing a premature STOP codon in strain SC5314 compared to Muzzey et al. (10) could be explained by the stringency of our analysis. Indeed, only positions with high SNP quality and coverage depth of >20 for all 182 strains of our collection were considered for further analysis.

A promising candidate to explain the homozygosity bias observed for Chr1 is the *gcd6** allele (C1_08600C_B) that carries a SNP introducing a premature STOP codon, truncating the protein from the 17 C-terminal amino acids. In *S. cerevisiae*, *GCD6* encodes the catalytic epsilon subunit of the translation initiation factor eIF2B. The truncated domain is found at the C terminus of several translation initiation factors and is important for mediating protein-protein interactions. *GCD6* is essential in *S. cerevisiae*, as null mutants are not viable. The same is likely to be true in *C. albicans*, since heterozygous mutants are viable, but null mutants have not been reported in the literature. Therefore, it can be hypothesized that homozygosity of *gcd6**, located on Chr1B, could result in cell death and be responsible for the homozygosity bias observed on Chr1 (Table 1).

Interestingly, a recent transposon mutagenesis screen in haploid *C. albicans* also argues that *CaGCD6* is essential (30). Among the 12 candidate RLAs presented in Table 2, the same screen argues for essentiality of *CaGPI16* (previously identified by Feri et al. [13]) and *CaMTR4* (identified in this study). Although the 10 remaining genes in Table 2 were defined as nonessential genes by Segal et al. (30), it is puzzling to see that the mutated alleles with a premature STOP codon were never observed in the homozygous state in the natural population of 182 *C. albicans* isolates. This observation highlights the complementarity of the study by Segal et al. (30) and our work, given that gene essentiality can vary depending on growth conditions and *in vitro* assessment of gene essentiality does not necessarily correlate with *in vivo* essentiality.

From a mechanistic point of view, our work revealed that most of the cells that have undergone an I-SceI-mediated DNA DSB on Chr7 use gene conversion as a repair mechanism, thus limiting LOH extent and the loss of genetic information. Break-induced replication, mitotic crossover, gene conversion with crossover and chromosome truncation that lead to long-range LOH events in decreasing order are less frequently utilized. Our results are consistent with those of Feri et al. (13) on Chr4, arguing that our observation is not locus specific but can be applied genome-wide in

TABLE 2 Genome-wide RLA candidates in the *C. albicans* strain SC5314^a

Chr	Position	ORF name	Gene name	Description	Haplotype of mutated allele	Essentiality in:	
						<i>C. albicans</i>	<i>S. cerevisiae</i>
Ca22chr1A	1131425	C1_05380C_A		Ortholog(s) have telomeric DNA binding activity, role in DNA double-strand break processing, DNA replication initiation, chromatin silencing at silent mating-type cassette, telomere capping, and shelterin complex localization	B	No info	No
Ca22chr1A	1760072	C1_08070W_A	CDR4	Putative ABC transporter superfamily; fluconazole, Sfu1, Hog1, core stress response induced; caspofungin repressed; fluconazole resistance not affected by mutation or correlated with expression; rat catheter and flow model biofilm induced	B	No	No
Ca22chr1A	1882812	C1_08600C_A	GCD6	Ortholog of <i>S. cerevisiae</i> Gcd6; catalytic epsilon subunit of the translation initiation factor eIF2B; genes encoding translation factors are repressed by phagocytosis by murine macrophages	B	Het ok	Yes
Ca22chr1A	1986384	C1_09100W_A	ZCF28	Zn(II)2Cys6 transcription factor; required for yeast cell adherence to silicone substrate; Spider biofilm induced	A	No	No
Ca22chr1B	634346	C1_03040W_B		Protein of unknown function; induced by nitric oxide; rat catheter and Spider biofilm induced	A	No info	No
Ca22chr1B	834720	C1_03960C_B		Ortholog(s) have role in TOR signaling, reentry into mitotic cell cycle after pheromone arrest and endoplasmic reticulum membrane, endoplasmic reticulum-Golgi intermediate compartment localization	A	No	No
Ca22chr4A	659155	C4_03130W_A		Putative GPI transamidase component; possibly an essential gene, disruptants not obtained by UAU1 method	B	Het ok (no UAU mutant)	Yes
Ca22chr4A	796679	C4_03750C_A		Ortholog(s) have translation release factor activity, role in mitochondrial translational termination and mitochondrial inner membrane localization	B	No info	No
Ca22chr4B	531082	C4_02560C_B	UME7	Putative transcription factor with zinc cluster DNA binding motif; similar to <i>S. cerevisiae</i> Ume6p, which is a transcription factor involved in the regulation of meiotic genes	No allelic variation in feature	No	No
Ca22chr7A	746359	C7_03400C_A		Ortholog of <i>S. cerevisiae</i> Mtr4, an ATP-dependent 3'-5' RNA helicase of the DEAD box family; Hap43-induced gene; Spider biofilm induced	B	Het ok	Yes
Ca22chrRA	1603863	CR_07380C_A	KSR1	3-Ketosphinganine reductase, catalyzes the second step in phytosphingosine synthesis	B	No	Yes
Ca22chrRA	1782353	CR_08200C_A		Putative MRP/CFTR-subfamily ABC transporter; member of multidrug resistance-associated protein (MRP) subfamily of ABC family; similar to <i>S. cerevisiae</i> Bpt1p	B	Het ok	No

^aConfirmed RLAs are indicated by medium gray shading (reference 13 and this study), and the recessive deleterious allele is indicated by light gray shading (13).

C. albicans. However, we cannot exclude the possibility that the relative usage of these repair mechanisms is specific to I-SceI-induced DNA DSB, i.e., DNA DSBs induced by the CRISPR-Cas9 RNA-guided endonuclease could be preferentially handled by another mechanism of DNA repair.

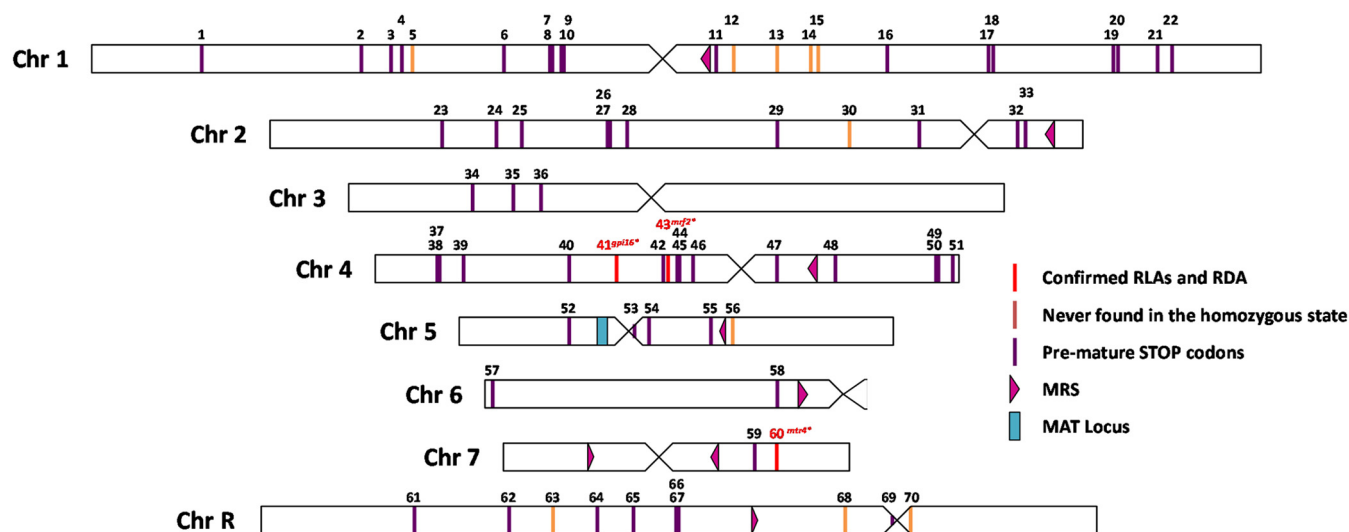


FIG 4 Schematic representation of the localization of premature STOP-inducing SNPs in the *C. albicans* SC5314 genome. Representation of 70 heterozygous SNPs (vertical bars) inducing a premature STOP codon distributed on all eight chromosomes of the reference strain SC5314. SNPs inducing premature STOP codons that are never found in the homozygous state in the library of 182 genomes of clinical *C. albicans* isolates are represented in orange, while confirmed recessive lethal and deleterious alleles are identified in red. Details regarding each SNP can be found in Table S1 using the assigned numbers in this figure.

In the course of this study, we also addressed the role that repetitive sequences, such as MRS, might play on the overall genome dynamics of *C. albicans*. This was achieved by studying how MRS position affects the outcome of I-SceI-induced LOH. Even though most *C. albicans* chromosomes possess a unique MRS region, the presence of two MRS regions, one on each arm, is unique to Chr7 (19). We observed that the presence of *mrs-7b* or *mrs-7a* between the I-SceI TS and the telomere-proximal LOH reporter system on Chr7 results in equal augmentation of the mono-BFP and mono-GFP populations upon I-SceI-dependent DNA DSB (Fig. 3). This contrasts with what is observed when the I-SceI TS is located downstream of the MRS, whereby the monofluorescent population arising by break-induced replication or mitotic crossover is increased relative to the monofluorescent population arising by gene conversion with crossover in the G₂ phase of the cell cycle (a scarce molecular mechanism), unless a RLA is present. This suggests that the MRS could be a hot spot for interhomolog mitotic crossover on Chr7. Indeed, upon recombination events at the MRS, DSBs repaired by break-induced replication or mitotic crossover would result in a relatively equal appearance of both monofluorescent populations when I-SceI-TS is located between the centromere and the MRS (Fig. 3B and C).

Mitotic crossovers at MRS could be an intrinsic feature of these repeat regions or be triggered by either (i) stress resulting from I-SceI overexpression or (ii) the physical I-SceI-induced DNA DSB. The former would imply that increased mitotic crossovers at MRS should be expected on all chromosomes remaining to be tested. The latter would imply that increased mitotic crossovers at Chr7 MRS are observed only upon repair of a DNA DSB upstream of these repeated regions. These latter hypotheses are consistent with a role for stress in the enhancement of the recombination frequency near the MRS or in general, as already suggested by Lephart et al. (20). Importantly, our results confirm the original proposal of Pujol et al. (31) that MRS on Chr7 are hot spots for recombination. Concretely, MRS would allow switching *C. albicans* haplotypes by generating a new combination of alleles. Information regarding the biological importance of MRS remains scarce despite the positive selection on MRS leading to the maintenance of these large and unique repeats in the *C. albicans* genome. Such recombination events provide *C. albicans* with increased opportunities to survive DNA DSBs whose repair can lead to homozygosis of recessive lethal or deleterious alleles. This might explain the maintenance of MRS in this species.

TABLE 3 *C. albicans* strains used in this study

Strain	Genotype	Characteristic	Auxotrophies	Parental strain	Reference
CEC4591	<i>arg4Δ/arg4Δ his1Δ/his1Δ ura3Δ::λimm434/ura3Δ::λimm434 iro1Δ::λimm434/iro1Δ::λimm434 ADH1/adh1::PTDH3-carTA::SAT1</i> Ca21chr1_C_ <i>albicans</i> _SC5314:625304 to 626436Δ::ClpXH-HYGb-PTET-ATG-NLS-I-SceI/Ca21chr1_C_ <i>albicans</i> _SC5314:625304 to 626436	pNIMx-pTet-NLS-I-SceI	arg ⁻ his ⁻ uri ⁻ HygR NsnR	CEC1448	13
CEC4679	<i>arg4Δ/arg4Δ his1Δ/his1Δ ura3Δ::λimm434/ura3Δ::λimm434 iro1Δ::λimm434/iro1Δ::λimm434 ADH1/adh1::PTDH3-carTA::SAT1</i> Ca21chr1_C_ <i>albicans</i> _SC5314:625304 to 626436Δ::ClpXH-HYGb-PTET-ATG-NLS-I-SceI/Ca21chr1_C_ <i>albicans</i> _SC5314:625304 to 626436 Ca22chr7_C_ <i>albicans</i> _SC5314:911053 to 911347::PTDH3-GFP-CdARG4	CEC4591 + Ch7Right_pTDH3-ARG4-GFP	ARG ⁺ his ⁻ uri ⁻ NsnR HygR	CEC4591	This study
CEC4685	<i>arg4Δ/arg4Δ his1Δ/his1Δ ura3Δ::λimm434/ura3Δ::λimm434 iro1Δ::λimm434/iro1Δ::λimm434 ADH1/adh1::PTDH3-carTA::SAT1</i> Ca21chr1_C_ <i>albicans</i> _SC5314:625304 to 626436Δ::ClpXH-HYGb-PTET-ATG-NLS-I-SceI/Ca21chr1_C_ <i>albicans</i> _SC5314:625304 to 626436 Ca22chr7_C_ <i>albicans</i> _SC5314:911053 to 911347::PTDH3-GFP-CdARG4/PTDH3-BFP-CdHIS1	CEC4679 + Chr7Right_pTDH3-HIS1-BFP	ARG ⁺ HIS ⁺ uri ⁻ NsnR HygR	CEC4679	This study
CEC4818	<i>arg4Δ/arg4Δ his1Δ/his1Δ ura3Δ::λimm434/ura3Δ::λimm434 iro1Δ::λimm434/iro1Δ::λimm434 ADH1/adh1::PTDH3-carTA::SAT1</i> Ca21chr1_C_ <i>albicans</i> _SC5314:625304 to 626436Δ::ClpXH-HYGb-PTET-ATG-NLS-I-SceI/Ca21chr1_C_ <i>albicans</i> _SC5314:625304 to 626436 Ca22chr7_C_ <i>albicans</i> _SC5314:911053 to 911347::PTDH3-GFP-CdARG4/PTDH3-BFP-CdHIS1 Ca22chr7_C_ <i>albicans</i> _SC5314:446552 to 446704::PTDH3-CdURA3-I-SceI-TS	CEC4685 + relocated I-SceI TS on HapA	ARG ⁺ HIS ⁺ URI ⁺ NsnR HygR	CEC4685	This study
CEC4819	<i>arg4Δ/arg4Δ his1Δ/his1Δ ura3Δ::λimm434/ura3Δ::λimm434 iro1Δ::λimm434/iro1Δ::λimm434 ADH1/adh1::PTDH3-carTA::SAT1</i> Ca21chr1_C_ <i>albicans</i> _SC5314:625304 to 626436Δ::ClpXH-HYGb-PTET-ATG-NLS-I-SceI/Ca21chr1_C_ <i>albicans</i> _SC5314:625304 to 626436 Ca22chr7_C_ <i>albicans</i> _SC5314:911053 to 911347::PTDH3-GFP-CdARG4/PTDH3-BFP-CdHIS1 Ca22chr7_C_ <i>albicans</i> _SC5314:446552 to 446704::PTDH3-CdURA3-I-SceI-TS	CEC4685 + relocated I-SceI TS on HapB	ARG ⁺ HIS ⁺ URI ⁺ NsnR HygR	CEC4685	This study
CEC5061	<i>arg4Δ/arg4Δ his1Δ/his1Δ ura3Δ::λimm434/ura3Δ::λimm434 iro1Δ::λimm434/iro1Δ::λimm434 ADH1/adh1::PTDH3-carTA::SAT1</i> Ca21chr1_C_ <i>albicans</i> _SC5314:625304 to 626436Δ::ClpXH-HYGb-PTET-ATG-NLS-I-SceI/Ca21chr1_C_ <i>albicans</i> _SC5314:625304 to 626436 Ca22chr7_C_ <i>albicans</i> _SC5314:911053 to 911347::PTDH3-GFP-CdARG4/PTDH3-BFP-CdHIS1 Ca22chr7_C_ <i>albicans</i> _SC5314:725867 to 726122::PTDH3-CdURA3-I-SceI-TS	CEC4685 + I-SceI TS on HapA	ARG ⁺ HIS ⁺ URI ⁺ NsnR HygR	CEC4685	This study
CEC5062	<i>arg4Δ/arg4Δ his1Δ/his1Δ ura3Δ::λimm434/ura3Δ::λimm434 iro1Δ::λimm434/iro1Δ::λimm434 ADH1/adh1::PTDH3-carTA::SAT1</i> Ca21chr1_C_ <i>albicans</i> _SC5314:625304 to 626436Δ::ClpXH-HYGb-PTET-ATG-NLS-I-SceI/Ca21chr1_C_ <i>albicans</i> _SC5314:625304 to 626436 Ca22chr7_C_ <i>albicans</i> _SC5314:911053 to 911347::PTDH3-GFP-CdARG4/PTDH3-BFP-CdHIS1 Ca22chr7_C_ <i>albicans</i> _SC5314:725867 to 726122::PTDH3-CdURA3-I-SceI-TS	CEC4685 + I-SceI TS on HapB	ARG ⁺ HIS ⁺ URI ⁺ NsnR HygR	CEC4685	This study
CEC5067	<i>arg4Δ/arg4Δ his1Δ/his1Δ ura3Δ::λimm434/ura3Δ::λimm434 iro1Δ::λimm434/iro1Δ::λimm434 ADH1/adh1::PTDH3-carTA::SAT1</i> Ca21chr1_C_ <i>albicans</i> _SC5314:625304 to 626436Δ::ClpXH-HYGb-PTET-ATG-NLS-I-SceI/Ca21chr1_C_ <i>albicans</i> _SC5314:625304 to 626436 Ca22chr7_C_ <i>albicans</i> _SC5314:911053 to 911347::PTDH3-GFP-CdARG4/PTDH3-BFP-CdHIS1 Ca22chr7_C_ <i>albicans</i> _SC5314:446552 to 446704::PTDH3-CdURA3-I-SceI-TS RPS1::Clp10/RPS1::PTDH3-MTR4-IMH3r	CEC4818 + pTDH3-IMH3-MTR4	ARG ⁺ HIS ⁺ URI ⁺ NsnR HygR MpaR	CEC4818	This study

(Continued on next page)

TABLE 3 (Continued)

Strain	Genotype	Characteristic	Auxotrophies	Parental strain	Reference
CEC5072	<i>arg4Δ/arg4Δ his1Δ/his1Δ ura3Δ::λimm434/ura3Δ::λimm434 iro1Δ::λimm434/iro1Δ::λimm434 ADH1/adh1::PTDH3-carTA::SAT1Ca21chr1_C_albicans_SC5314:625304 to 626436Δ::ClpXH-HYGb-PTET-ATG-NLS-I-SceI/Ca21chr1_C_albicans_SC5314:625304 to 626436 Ca22chr7_C_albicans_SC5314:911053 to 911347::PTDH3-GFP-CdARG4/PTDH3-BFP-CdHIS1 Ca22chr7_C_albicans_SC5314:446552 to 446704::PTDH3-CdURA3-I-SceI-TS RPS1::Clp10/RPS1::PTDH3-MTR4-IMH3r</i>	CEC4819 + pTDH3-IMH3-MTR4	ARG+ HIS+ URI+ NsnR HygR MpaR	CEC4819	This study
CEC5075	<i>arg4Δ/arg4Δ his1Δ/his1Δ ura3Δ::λimm434/ura3Δ::λimm434 iro1Δ::λimm434/iro1Δ::λimm434 ADH1/adh1::PTDH3-carTA::SAT1Ca21chr1_C_albicans_SC5314:625304 to 626436Δ::ClpXH-HYGb-PTET-ATG-NLS-I-SceI/Ca21chr1_C_albicans_SC5314:625304 to 626436 Ca22chr7_C_albicans_SC5314:911053 to 911347::PTDH3-GFP-CdARG4/PTDH3-BFP-CdHIS1 Ca22chr7_C_albicans_SC5314:725867 to 726122::PTDH3-CdURA3-I-SceI-TS RPS1::Clp10/RPS1::PTDH3-MTR4-IMH3r</i>	CEC5061 + pTDH3-IMH3-MTR4	ARG+ HIS+ URI+ NsnR HygR MpaR	CEC5061	This study
CEC5078	<i>arg4Δ/arg4Δ his1Δ/his1Δ ura3Δ::λimm434/ura3Δ::λimm434 iro1Δ::λimm434/iro1Δ::λimm434 ADH1/adh1::PTDH3-carTA::SAT1 Ca21chr1_C_albicans_SC5314:625304 to 626436Δ::ClpXH-HYGb-PTET-ATG-NLS-I-SceI/Ca21chr1_C_albicans_SC5314:625304 to 626436 Ca22chr7_C_albicans_SC5314:911053 to 911347::PTDH3-GFP-CdARG4/PTDH3-BFP-CdHIS1 Ca22chr7_C_albicans_SC5314:725867 to 726122::PTDH3-CdURA3-I-SceI-TS RPS1::Clp10/RPS1::PTDH3-MTR4-IMH3r</i>	CEC5062 + pTDH3-IMH3-MTR4	ARG+ HIS+ URI+ NsnR HygR MpaR	CEC5062	This study

MATERIALS AND METHODS

Strains and media. *C. albicans* strains used in this work are derived from the reference strain SC5314. The cloning experiments were carried out using One Shot TOP10 chemically competent *Escherichia coli* cells (ThermoFisher Scientific). All *C. albicans* strains and *E. coli* plasmids generated and used throughout this investigation are listed in Table 3 and Table S2 in the supplemental material, respectively.

C. albicans cells were maintained on rich yeast extract-peptone-dextrose (YPD) medium (1% yeast extract, 2% peptone, 2% dextrose). Synthetic complete (SC) (0.67% yeast nitrogen base without amino acids, 2% dextrose, 0.08% drop out mix) and synthetic defined (SD) (0.67% yeast nitrogen base without amino acids, 2% dextrose) media, both with drop out amino acids, depending on auxotrophy of the strains, were used as selective media. Solid media were obtained by adding 2% agar. 5-Fluoroorotic acid (5-FOA)-containing agar medium (0.67% yeast nitrogen base without amino acid, 0.0625% 5-fluoroorotic acid [Toronto Research Chemicals], 0.01% uridine, 2% glucose, 2% agar supplemented with arginine and histidine) was used to detect cells that have a nonfunctional *URA3* gene. Mycophenolic acid (MPA) medium is composed of SD medium with 5 μg/ml MPA (Sigma-Aldrich). Meanwhile, *E. coli* strains were cultured on/in LB or 2YT medium, with appropriate antibiotics for selection purposes (kanamycin [50 μg/ml], ticarcillin [50 μg/ml], and gentamicin [10 μg/ml]).

In silico identification of potential recessive lethal alleles. A collection of 182 *C. albicans* genomes (7) was utilized with the intention to search for potential RLAs. SNPs were compiled and filtered with the following criteria: (i) an SNP that introduces a premature STOP codon in a coding region (open reading frame [ORF]), (ii) this SNP was never observed in the homozygous state, (iii) the SNP lies in a coding region never found to be dispensable in *C. albicans*, and (iv) the SNP was found in the heterozygous state in the reference strain SC5314.

Plasmid constructions. Methods for the construction of plasmids used for I-SceI target sequence (TS) insertion (pFA-*URA3-I-SceI-TS-HSP90/CUP9*) and for complementation with the wild-type *MTR4* allele (Clp10-*P_{TDH3}-MTR4-IMH3*) are described in Text S1 in the supplemental material.

***C. albicans* strain constructions.** Construction of strain CEC4685 is described in Text S1. Briefly, this strain is derived from the common laboratory strain SN76 and carries the I-SceI-encoding gene under the control of the inducible *P_{TET}* promoter (32), pNIMX coding for the transactivator necessary for activation of the *P_{TET}* promoter in the presence of tetracycline derivatives (33), and the BFP/GFP LOH reporter system (15) on the right arm of Chr7. Integration of the I-SceI TS was achieved by transformation of strain CEC4685 with a PCR-amplified cassette bearing the I-SceI TS and Chr7 homology regions, the latter borne from primers 9 and 10 (Table S3) used in amplification of pFA-*URA3-I-SceI-TS-CDR3/TG(GCC)2* (13). This led to prototroph strains named CEC5061 (I-SceI TS on HapA) and CEC5062 (I-SceI TS on HapB) (Table 3).

Relocalization of I-SceI TS upstream of the MRS was conducted by transforming strain CEC4685 with *HpaI*+*ScalI*-cut plasmid of pFA-*URA3-I-SceI-TS-HSP90/CUP9*, which carries the *URA3-I-SceI* TS construction for integration on Chr7. The now prototroph transformants were selected on SD medium. The final strains were named CEC4818 (I-SceI TS on HapA) and CEC4819 (I-SceI TS on HapB) (Table 3).

Strains possessing the BFP/GFP LOH reporter system on the left arm of Chr7 were generated by positioning the heterozygous BFP/GFP locus close to the left telomere (position 108,458 to 108,838) and the I-SceI TS at position 367,060 to 367,145 between *mrs-7a* (position 228,342 to 242,083) and the centromere (position 425,808 to 428,708).

Complementation of strains CEC5061, CEC5062, CEC4818, and CEC4819 with the wild-type *MTR4* allele at the *RPS1* locus was achieved using the *Stul*-linearized Clp10- P_{TDH3} -*MTR4-IMH3* plasmid described in Text S1. Transformants were selected on SD medium containing 5 μ g/ml MPA (Sigma-Aldrich), and the final strains were named CEC5067, CEC5072, CEC5075, and CEC5078, respectively (Table 3).

Following each transformation step, junction PCRs were conducted to ensure proper integrations. Additional controls were conducted such as fluorescence check (flow cytometry of 20,000 cells) and auxotrophy testing of strains (by spotting on SD supplemented with either Arg, His, Ura, or MPA). To ensure that the strains generated in the course of this study did not display growth defects resulting from transformation events, growth curves were generated using a TECAN Sunrise with OD readings (620 nm) every 10 min for a period of 48 h. Doubling times were outputted from the generated OD values and analyzed using GraphPad Prism 5.

Induction of the Tet-On system. In order to activate the Tet-On promoter and achieve I-SceI protein production, single colonies were precultured in liquid SC-His-Arg medium at 30°C. After overnight growth, induction was conducted in YPD plus anhydrotetracycline (ATc) (3 μ g/ml) (ThermoFisher ACROS Organics) for 8 h at 30°C, followed by an overnight recovery in YPD.

5-Fluoroorotic acid selection. Following the I-SceI induction protocol, as seen above, three different cell dilutions of cultures (20,000 cells, 2,000 cells, and 200 cells) grown in the presence (induced) or absence (noninduced; control) of ATc were plated on 5-fluoroorotic acid (5-FOA)-containing plates in triplicates. Dilutions were verified by plating a volume corresponding to 100 cells on YPD plates. The plates were incubated at 30°C for 3 days before analysis.

Cell preparation for flow cytometry and analysis. All flow cytometry analyses were conducted on the MACSQuant analyzer (Miltenyi Biotec) where BFP is detected with a 405-nm laser and 425- to 475-nm filters and GFP is detected with a 488-nm laser and 500- to 550-nm filters. Data for a maximum of 10⁶ cells were analyzed using the FlowJo V10.1 software. The gates to determine the LOH frequencies were arbitrarily selected but conserved throughout sample analysis.

Cell sorting. Induced and noninduced cultures were filtered using BD Falcon Cell strainers in order to remove large debris and filamentous cells that could obstruct the tubing system of the cytometer. The MoFlo Astrios flow cytometer was used to analyze and sort the cells of interest. For each sorted gate, 1,000 cells were recovered in 400 μ l of liquid YPD medium, plated immediately after cell sorting on four YPD petri plates, and incubated at 30°C for 48 h before collection of results.

SNP-RFLP. *In silico* identification of heterozygous SNPs affecting a restriction site on only one haplotype of Chr7 was used for haplotype characterization of strains. First, a nucleotide multiple sequence alignment by MUSCLE was conducted using the Chr7A and Chr7B sequences from the reference strain SC5314 (22). Heterozygous SNPs were selected using the following criteria. (i) It interrupts a commonly known restriction site on one haplotype. (ii) The selected enzyme does not cut again within a range of 1 kb. (iii) The heterozygous SNP is present in most strains of the collection of 182 *C. albicans* clinical strains (7). Second, primer pairs were designed to result in PCR products with different digestion profiles and used to verify the presence of the heterozygous SNP in our strain of interest.

These SNPs were used for two distinct purposes: (i) to assign the Chr7 homolog targeted by I-SceI TS integration and (ii) to monitor the heterozygous status of the left and right arms of Chr7 upon DNA DSB repair. Regions of roughly 2.5 kb surrounding the heterozygous SNPs were amplified by PCR and digested with the appropriate restriction enzyme overnight. *C. albicans* gDNA extractions, PCRs, and amplicon verifications were conducted following the methods of Feri et al. (13), while a list of the primers used can be found in Table S3. The SNPs at positions 444,929 (*Bgl*II cutting HapA) and 727,328 (*Hpa*I cutting HapA) were used to identify the I-SceI-targeted haplotype of the right arm of Chr7, when the I-SceI TS is located upstream and downstream of the *mrs-7b*, respectively. The 2.2-kb and 2.16-kb regions around the heterozygous SNPs located at positions 414,508 (left arm) and 744,964 (right arm) utilizing *Att*I (cutting HapB) and *Hae*III (cutting HapB) enzymes, respectively, were used to assess the heterozygous status of both Chr7 arms. All SNP-RFLP sites and the enzyme-sensitive haplotypes are summarized in Fig. S1.

SUPPLEMENTAL MATERIAL

Supplemental material for this article may be found at <https://doi.org/10.1128/mSphere.00709-18>.

TEXT S1, DOCX file, 0.05 MB.

FIG S1, TIF file, 0.1 MB.

FIG S2, TIF file, 0.5 MB.

TABLE S1, DOCX file, 0.04 MB.

TABLE S2, DOCX file, 0.03 MB.

TABLE S3, DOCX file, 0.03 MB.

ACKNOWLEDGMENTS

T.M. is the recipient of a Ph.D. fellowship from the Laboratoire d'Excellence Integrative Biology of Emerging Infectious Diseases (ANR-10-LABX-62-IBEID). A.F. was the recipient of a Ph.D. fellowship from INRA and Institut Pasteur. We acknowledge support from the French Government's Investissement d'Avenir program (Laboratoire d'Excellence Integrative Biology of Emerging Infectious Diseases [ANR-10-LABX-62-IBEID]).

REFERENCES

- Gerstein AC, Kuzmin A, Otto SP. 2014. Loss-of-heterozygosity facilitates passage through Haldane's sieve for *Saccharomyces cerevisiae* undergoing adaptation. *Nat Commun* 5:3819. <https://doi.org/10.1038/ncomms4819>.
- Coste A, Selmecki A, Forche A, Diogo D, Bougnoux M-E, d'Enfert C, Berman J, Sanglard D. 2007. Genotypic evolution of azole resistance mechanisms in sequential *Candida albicans* isolates. *Eukaryot Cell* 6:1889–1904. <https://doi.org/10.1128/EC.00151-07>.
- Selmecki A, Forche A, Berman J. 2006. Aneuploidy and isochromosome formation in drug-resistant *Candida albicans*. *Science* 313:367–370. <https://doi.org/10.1126/science.1128242>.
- Prieto D, Correia I, Pla J, Román E. 2016. Adaptation of *Candida albicans* to commensalism in the gut. *Future Microbiol* 11:567–583. <https://doi.org/10.2217/fmb.16.1>.
- Jones T, Federspiel NA, Chibana H, Dungan J, Kalman S, Magee BB, Newport G, Thorstenson YR, Agabian N, Magee PT, Davis RW, Scherer S. 2004. The diploid genome sequence of *Candida albicans*. *Proc Natl Acad Sci U S A* 101:7329–7334. <https://doi.org/10.1073/pnas.0401648101>.
- Hirakawa MP, Martinez DA, Sakthikumar S, Anderson MZ, Berlin A, Gujja S, Zeng Q, Zisson E, Wang JM, Greenberg JM, Berman J, Bennett RJ, Cuomo CA. 2015. Genetic and phenotypic intra-species variation in *Candida albicans*. *Genome Res* 25:413–425. <https://doi.org/10.1101/gr.174623.114>.
- Ropars J, Maufrais C, Diogo D, Marcet-Houben M, Perin A, Sertour N, Mosca B, Peral E, Laval G, Bouchier C, Ma L, Schwartz K, Voelz K, May RC, Poulain J, Batail C, Wincker P, Borman AM, Chowdhary A, Fan S, Kim SH, Le Pape P, Romeo O, Shin JH, Gabaldon T, Sherlock G, Bougnoux M-E, d'Enfert C. 2018. Gene flow contributes to diversification of the major fungal pathogen *Candida albicans*. *Nat Commun* 9:2253. <https://doi.org/10.1038/s41467-018-04787-4>.
- Hickman MA, Zeng G, Forche A, Hirakawa MP, Abbey D, Harrison BD, Wang Y-M, Su C, Bennett RJ, Wang Y, Berman J. 2013. The 'obligate diploid' *Candida albicans* forms mating-competent haploids. *Nature* 494: 55–59. <https://doi.org/10.1038/nature11865>.
- Abbey DA, Funt J, Lurie-Weinberger MN, Thompson DA, Regev A, Myers CL, Berman J. 2014. YMAP: a pipeline for visualization of copy number variation and loss of heterozygosity in eukaryotic pathogens. *Genome Med* 6:1–16. <https://doi.org/10.1186/s13073-014-0100-8>.
- Muzzey D, Schwartz K, Weissman JS, Sherlock G. 2013. Assembly of a phased diploid *Candida albicans* genome facilitates allele-specific measurements and provides a simple model for repeat and indel structure. *Genome Biol* 14:R97. <https://doi.org/10.1186/gb-2013-14-9-r97>.
- Gómez-Raja J, Andaluz E, Magee B, Calderone R, Larriba G. 2008. A single SNP, G929T (Gly310Val), determines the presence of a functional and a non-functional allele of *HIS4* in *Candida albicans* SC5314: detection of the non-functional allele in laboratory strains. *Fungal Genet Biol* 45: 527–541. <https://doi.org/10.1016/j.fgb.2007.08.008>.
- Ciudad T, Hickman M, Bellido A, Berman J, Larriba G. 2016. Phenotypic consequences of a spontaneous loss of heterozygosity in a common laboratory strain of *Candida albicans*. *Genetics* 203:1161–1176. <https://doi.org/10.1534/genetics.116.189274>.
- Feri A, Loll-Krippelber R, Commere P-H, Maufrais C, Sertour N, Schwartz K, Sherlock G, Bougnoux M-E, D'Enfert C, Legrand M. 2016. Analysis of repair mechanisms following an induced double strand break uncovers recessive deleterious alleles in the *Candida albicans* diploid genome. *mBio* 7:e01109-16. <https://doi.org/10.1128/mBio.01109-16>.
- Muzzey D, Sherlock G, Weissman JS. 2014. Extensive and coordinated control of allele-specific expression by both transcription and translation in *Candida albicans*. *Genome Res* 24:963–973. <https://doi.org/10.1101/gr.166322.113>.
- Loll-Krippelber R, Feri A, Nguyen M, Maufrais C, Yansouni J, d'Enfert C, Legrand M. 2015. A FACS-optimized screen identifies regulators of genome stability in *Candida albicans*. *Eukaryot Cell* 14:311–322. <https://doi.org/10.1128/EC.00286-14>.
- Malkova A, Klein F, Leung W-Y, Haber JE. 2000. HO endonuclease-induced recombination in yeast meiosis resembles Spo11-induced events. *Proc Natl Acad Sci U S A* 97:14500–14505. <https://doi.org/10.1073/pnas.97.26.14500>.
- Forche A, Alby K, Schaefer D, Johnson AD, Berman J, Bennett RJ. 2008. The parasexual cycle in *Candida albicans* provides an alternative pathway to meiosis for the formation of recombinant strains. *PLoS Biol* 6:e110. <https://doi.org/10.1371/journal.pbio.0060110>.
- Andaluz E, Bellido A, Gómez-Raja J, Selmecki A, Bouchonville K, Calderone R, Berman J, Larriba G. 2011. Rad52 function prevents chromosome loss and truncation in *Candida albicans*. *Mol Microbiol* 79:1462–1482. <https://doi.org/10.1111/j.1365-2958.2011.07532.x>.
- Chibana H, Magee PT. 2009. The enigma of the major repeat sequence of *Candida albicans*. *Future Microbiol* 4:171–179. <https://doi.org/10.2217/17460913.4.2.171>.
- Lephart PR, Chibana H, Magee PT. 2005. Effect of the major repeat sequence on chromosome loss in *Candida albicans*. *Eukaryot Cell* 4:733–741. <https://doi.org/10.1128/EC.4.4.733-741.2005>.
- Kirsch DR, Whitney RR. 1991. Pathogenicity of *Candida albicans* auxotrophic mutants in experimental infections. *Infect Immun* 59:3297–3300.
- Skrzypek MS, Binkley J, Binkley G, Miyasato SR, Simison M, Sherlock G. 2017. The *Candida* Genome Database (CGD): incorporation of Assembly 22, systematic identifiers and visualization of high throughput sequencing data. *Nucleic Acids Res* 45:D592–D596. <https://doi.org/10.1093/nar/gkw924>.
- Giaever G, Chu AM, Ni L, Connelly C, Riles L, Véronneau S, Dow S, Lucau-Danila A, Anderson K, André B, Arkin AP, Astromoff A, El Bakkouri M, Bangham R, Benito R, Brachat S, Campanaro S, Curtiss M, Davis K, Deutschbauer A, Entian K-D, Flaherty P, Foury F, Garfinkel DJ, Gerstein M, Gotte D, Güldener U, Hegemann JH, Hempel S, Herman Z, Jaramillo DF, Kelly DE, Kelly SL, Kötter P, LaBonte D, Lamb DC, Lan N, Liang H, Liao H, Liu L, Luo C, Lussier M, Mao R, Menard P, Ooi SL, Revuelta JL, Roberts CJ, Rose M, Ross-Macdonald P, Scherens B, Schimmack G, et al. 2002. Functional profiling of the *Saccharomyces cerevisiae* genome. *Nature* 418:387. <https://doi.org/10.1038/nature00935>.
- Bernstein KA, Granneman S, Lee AV, Manickam S, Baserga SJ. 2006. Comprehensive mutational analysis of yeast DEXD/H box RNA helicases involved in large ribosomal subunit biogenesis. *Mol Cell Biol* 26: 1195–1208. <https://doi.org/10.1128/MCB.26.4.1195-1208.2006>.
- De Gobbi M, Viprakasit V, Hughes JR, Fisher C, Buckle VJ, Ayyub H, Gibbons RJ, Vernimmen D, Yoshinaga Y, de Jong P, Cheng J-F, Ruben EM, Wood WG, Bowden D, Higgs DR. 2006. A regulatory SNP causes a human genetic disease by creating a new transcriptional promoter. *Science* 312:1215–1217. <https://doi.org/10.1126/science.1126431>.
- Nackley AG, Shabalina SA, Tchivileva IE, Satterfield K, Korchynskiy O, Makarov SS, Maixner W, Diatchenko L. 2006. Human catechol-O-methyltransferase haplotypes modulate protein expression by altering mRNA secondary structure. *Science* 314:1930–1933. <https://doi.org/10.1126/science.1131262>.
- Liang S, Hitomi M, Hu YH, Liu Y, Tartakoff AM. 1996. A DEAD-box-family protein is required for nucleocytoplasmic transport of yeast mRNA. *Mol Cell Biol* 16:5139–5146. <https://doi.org/10.1128/MCB.16.9.5139>.
- Smith SB, Kiss DL, Turk E, Tartakoff AM, Andrusis ED. 2011. Pronounced and extensive microtubule defects in a *Saccharomyces cerevisiae* DIS3 mutant. *Yeast* 28:755–769. <https://doi.org/10.1002/yea.1899>.
- Mohr G, Del Campo M, Mohr S, Yang Q, Jia H, Jankowsky E, Lambowitz AM. 2008. Function of the C-terminal domain of the DEAD-box protein

- Mss116p analyzed *in vivo* and *in vitro*. *J Mol Biol* 375:1344–1364. <https://doi.org/10.1016/j.jmb.2007.11.041>.
30. Segal ES, Gritsenko V, Levitan A, Yadav B, Dror N, Steenwyk JL, Silberberg Y, Mielich K, Rokas A, Gow NAR, Kunze R, Sharan R, Berman J. 2018. Gene essentiality analyzed by *in vivo* transposon mutagenesis and machine learning in a stable haploid isolate of *Candida albicans*. *mBio* 9:e02048-18. <https://doi.org/10.1128/mBio.02048-18>.
 31. Pujol C, Joly S, Nolan B, Srikantha T, Soll DR. 1999. Microevolutionary changes in *Candida albicans* identified by the complex Ca3 fingerprinting probe involve insertions and deletions of the full-length repetitive sequence RPS at specific genomic sites. *Microbiology* 145:2635–2646. <https://doi.org/10.1099/00221287-145-10-2635>.
 32. Park Y-N, Morschhäuser J. 2005. Tetracycline-inducible gene expression and gene deletion in *Candida albicans*. *Eukaryot Cell* 4:1328–1342. <https://doi.org/10.1128/EC.4.8.1328-1342.2005>.
 33. Chauvel M, Nesseir A, Cabral V, Znaidi S, Goyard S, Bachellier-Bassi S, Firon A, Legrand M, Diogo D, Naulleau C, Rossignol T, d'Enfert C. 2012. A versatile overexpression strategy in the pathogenic yeast *Candida albicans*: identification of regulators of morphogenesis and fitness. *PLoS One* 7:e45912. <https://doi.org/10.1371/journal.pone.0045912>.